

Review Article

Thin film growth of MAX phases as functional materials

Abhijit Biswas^{1,*}, Varun Natu², and Anand B. Puthirath¹

¹Department of Materials Science and Nanoengineering, Rice University, Houston, TX 77005, USA

²Department of Materials Science & Engineering, Drexel University, Philadelphia, PA 19104, USA

ABSTRACT

Layered nanolaminate ternary carbides, nitrides and carbonitrides with general formula $M_{n+1}AX_n$ or MAX ($n = 1, 2, \text{ or } 3$, M is an early transition metal, A is mostly group 13 or 14 element, and X is C and/or N) has revolutionized the world of nanomaterials, due to the coexistence of both ceramic and metallic nature, giving rise to exceptional mechanical, thermal, electrical, chemical properties and wide range of applications. Although several solid-state bulk synthesis methods have been developed to produce a variety of MAX phases, however, for certain applications, the growth of MAX phases, especially in its high-quality epitaxial thin films form is of increasing interest. Here, we summarize the progress made thus far in epitaxial growth and property evaluation of MAX phase thin films grown by various deposition techniques. We also address the important future research directions to be made in terms of thin-film growth. Overall, in the future, high-quality single-phase epitaxial thin film growth and engineering of chemically diverse MAX phases may open up interesting new avenues for next-generation technology.

Keywords: layered materials; ternary MAX phases; thin films; epitaxy; emergent properties

Correspondence e-mail: **01abhijit@gmail.com, abhijit.biswas@rice.edu**

(ORCID: 0000-0002-3729-4802)

INTRODUCTION

Layered nanolaminate ternary carbides and nitrides with chemical formula $M_{n+1}AX_n$ or MAX ($n = 1, 2, \text{ or } 3$, M is an early transition metal, A is a group 13 or 14 element, and X is C and/or N) is a unique class of material showing a combination of both ceramic and metallic properties [1-3]. Because of this unique nature, nanolaminate MAX materials show high electrical and thermal conductivity, excellent mechanical properties e.g. high Young's modulus and Vickers hardness, low frictional coefficient, high oxidation resistance, high damage tolerance than other ceramics, high thermal shock resistance, corrosion resistance, electro-catalysis for renewable energy production and high radiation damage tolerance for space and nuclear applications [4, 5]. Generally, MAX forms a layered hexagonal crystal structure (space group $P6_3/mmc$), where layers of edge-shared M_6X -octahedra separated by a two-dimensional (2D) closed packed layers of "A" elements, which are located at the center of trigonal prisms forming an alternate stacking of M-X and A layers. Its high metallicity (low resistivity $\sim \mu\Omega\text{-cm}$) is due to the presence of a substantial amount of density of states at the Fermi level (E_F), with a dominant contribution coming from the $d-d$ orbitals of the M-element. The M-X bonds are extremely strong because of the presence of both covalent and metallic bonding nature, where M-A bonds are relatively weak, responsible for layered structure as well as a unique combination of both ceramic and metallic characteristics, thus bridging the gap between metals and ceramics. The MAX phase can be categorized further into 211 (M_2AX), 312 (M_3AX_2) and 413 (M_4AX_3) phases (Fig. 1). In 1963, the first discovery of the MAX phase was reported by Nowotny's group [6]. However, MAX remained largely unexplored for almost three decades, until the successful synthesis of bulk phase Ti_3SiC_2 MAX by Barsoum and El-Raghy [7], and henceforth ~ 160 new compounds have been synthesized in its bulk form, revolutionizing the world of layered functional carbides and nitrides nanomaterials [8].

One of the remarkable features of MAX is the conversion of it to MXene, formation of a new layered 2D material, analogue to graphene, showing a wide-range of functional properties and enormous potentials in almost every application sector [9]. 2D MXenes are typically obtained from 3D solid MAX via selective etching of A-layers by using fluoride ion containing acidic solutions. However, the surfaces of these layered 2D sheets are chemically terminated/functionalized with a different/selective group ($M_{n+1}X_nT_x$, where T_x is the surface termination) originating from the etchant, affecting the material properties extensively, e.g. electrical conductivity [10], and thus

hindering their usefulness for clean device fabrications for high-performance nano-electronics, embodying clean non-chemical fabrication protocols.

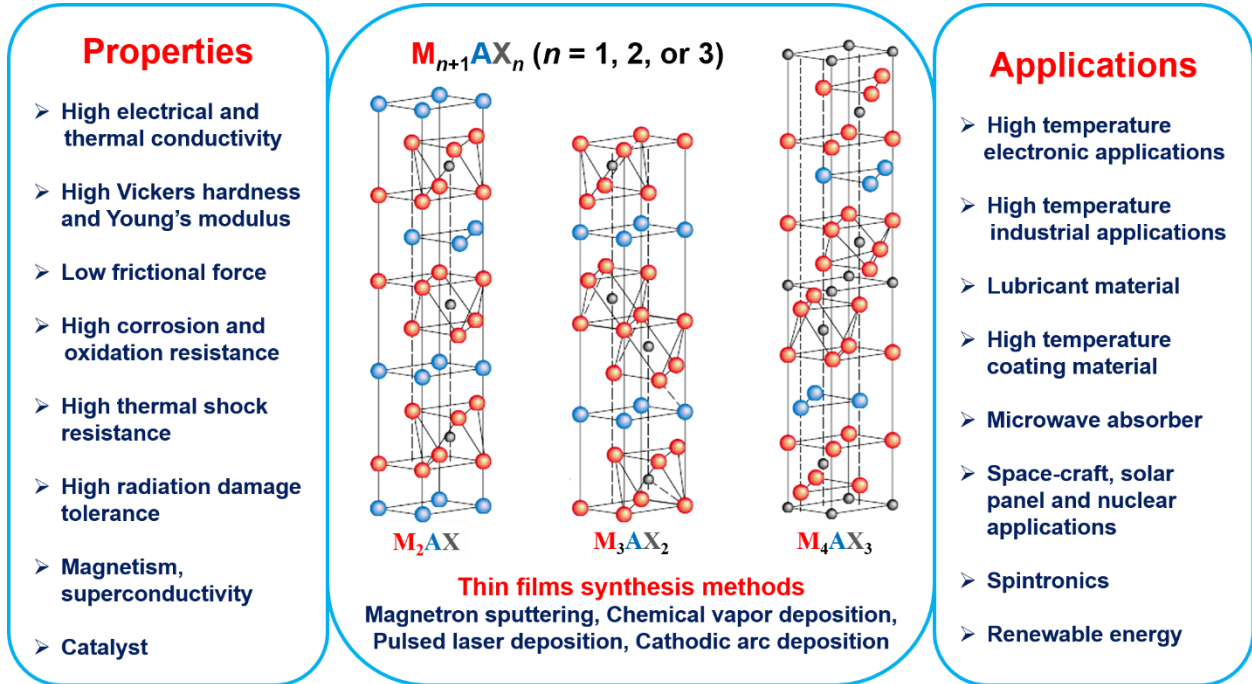


Figure 1: Layered ternary $M_{n+1}AX_n$ ($n = 1-3$) with a wide-range of properties and applications. The crystal structures were adapted with permission from Barsoum and El-Raghy, *American Scientist* 2001; **89**: 334, Copyright 2001 Sigma Xi, The Scientific Research Honor Society [2].

Although, a large numbers of layered bulk MAX phase compounds have been discovered (Table 1), as said however for relevant technological importance, the growth of MAX phases in its high-quality single-phase epitaxial thin film form of these films are highly desired. Therefore, in the last couple of decades, numerous attempts have been made to grow epitaxial MAX phase thin films by using various thin film growth methods and there are some review articles published along these directions [11-13]. Therefore, considering the growing interest about MAX phase thin films, in this article we attempt to summarize the progress made thus far in the growth and property evaluation of most, if not all the MAX phase thin films ($n = 1-3$). It was seen that epitaxial thin films also show excellent electrical, thermal, mechanical, tribological, magnetic, oxidation resistance, and corrosion properties with usefulness in high temperature based industrials applications, lubricant and coating materials, as well as radiation damage tolerance nuclear

materials, solar panels, and space-craft, making MAX based devices huge potential application worthiness. We also address several challenges and future explorations to be made in terms of thin film growth. Hence, growth and engineering of MAX phases especially in its high-quality epitaxial thin film form is important, showing unique functionalities and occasionally comparable or even suppressing the MXene properties, making MAX as next-generation application-worthy material.

Table 1: List of synthesized bulk $M_{n+1}AX_n$ ($n = 1-3$) compounds. This is an updated version of the earlier list provided by Sokol *et al.*, *Trends in Chemistry* 2019; **1**: 210 [8].

Phase	Materials
<p style="text-align: center;">211 (M₂AX)</p>	<p>Ti₂AlC, V₂AlC, Cr₂AlC, Nb₂AlC, Ta₂AlC, Zr₂AlC, Hf₂AlC, Ti₂GaC, V₂GaC, Cr₂GaC, Nb₂GaC, Mo₂GaC, Ta₂GaC, Mo₂AlC, Mo₂GaC, Mn₂GaC, Sc₂InC, Ti₂InC, Zr₂InC, Nb₂InC, Hf₂InC, Ti₂SnC, Zr₂SnC, V₂SnC, Nb₂SnC, Mo₂AuC, Nb₂CuC, Ti₂CdC, Sc₂InC, Ti₂InC, Zr₂InC, Nb₂InC, Hf₂InC, Ti₂TiC, Zr₂TiC, Hf₂TiC, Ti₂PbC, Zr₂PbC, Hf₂PbC, Ti₂GeC, V₂GeC, Cr₂GeC, Nb₂GeC, V₂PC, Nb₂PC, Ti₂SC, Zr₂SC, Nb₂SC_{0.4}, Nb₂SC, Hf₂SC, Ti₂ZnC, V₂ZnC, V₂AsC, Nb₂AsC, Ti₂GaN, Cr₂GaN, V₂GaN, Mo₂GaN, Ti₂InN, Zr₂InN, Hf₂SnN, Ti₂InN, Zr₂InN, Zr₂TiN, Ti₂AlN, Zr₂SeC, Ti₂AuN, Ti₂ZnN, (Cr,Mn)₂GaC, (Cr,Mn)₂GeC (Ti_{0.5}Nb_{0.5})₂AlC, (Ti_{0.5}V_{0.5})₂AlC, (Mo_{4/3}Y_{2/3})AlC, (Nb_{0.5}V_{0.5})₂AlC, (W_{2/3}Sc_{1/3})₂AlC, (W_{2/3}Y_{1/3})₂AlC, (Mo_{2/3}RE_{1/3})₂AlC (RE= Nd, Gd, Tb, Dy, Ho, and Er), Ti₂(Al_xCu_{1-x})N, V₂(A_xSn_{1-x})C (A = Fe, Co, Ni, Mn), (Ti_{1/5}V_{1/5}Zr_{1/5}Nb_{1/5}Ta_{1/5})₂AlC</p>
<p style="text-align: center;">312 (M₃AX₂)</p>	<p>Ti₃AlC₂, Ta₃AlC₂, Zr₃AlC₂, Ti₃SiC₂, Ti₃GaC₂, Ti₃GeC₂, Ti₃InC₂, Ti₃SnC₂, Zr₃SnC₂, Hf₃SnC₂, Ti₃AuC₂, Ti₃IrC₂, Ti₃ZnC₂, Ti₃ZnC₂, (Cr₂V)AlC₂, (Cr₂Ti)AlC₂, (Ti₂Zr)AlC₂, (Mo₂Se)AlC₂, (Mo₂Ti)AlC₂, (V,Mn)₃GaC₂ (V_{0.5}Cr_{0.5})₃AlC₂, (Zr_{0.5}Ti_{0.5})₃AlC₂, (Ti_{0.5}V_{0.5})₃AlC₂, (Cr_{2/3}Ti_{1/3})₃AlC₂, (Ta_{1-x}Ti_x)₃AlC₂, (Cr_{1/3}Ti_{2/3})₃AlC₂, Ti₃Al(C_{0.5}N_{0.5})₂, Ti₃(Al_xCu_{1-x})C₂</p>
<p style="text-align: center;">413 (M₄AX₃)</p>	<p>Ti₄SiC₃, Nb₄SiC₃, Ti₄AlN₃, Ta₄AlC₃, Nb₄AlC₃, V₄AlC₃, Ta₄GaC₃, Ti₄GaC₃, (Mo₂Ti₂)AlC₃, (Cr₂V₂)AlC₃, (V_{0.5}Cr_{0.5})₄AlC₃, (Nb_{0.5}V_{0.5})₄AlC₃, (Cr_{5/8}Ti_{3/8})₄AlC₃ (TiVNbMo)AlC₃, (TiVCrMo)AlC₃,</p>

THIN FILM GROWTH METHODS

Here we briefly summarize the various growth techniques that have been used for the deposition of MAX phases thin films. These are mainly chemical vapor deposition (CVD), magnetron sputtering, cathodic arc deposition, and pulsed laser deposition (PLD) [11]. In principle, each of these techniques has its own advantages and disadvantages. Generally, CVD requires very high temperature ($>1000\text{ }^{\circ}\text{C}$), however giving little success as several solution-based precursors are generally used, and leaving lots of residues on the surface. High power dc or radio frequency (rf) magnetron sputtering has been most often used to grow MAX phase films. Its advantage is that individual target sources are used to sputter, giving control over each element and the target compositions. In this technique films are grown typically at temperature $\sim 700\text{-}1000\text{ }^{\circ}\text{C}$ [11]. In some cases, reactive magnetron sputtering has also been employed to deposit the films by using N_2 as a source. The cathodic arc deposition technique has also been used to grow some MAX phase thin films. This method allows to grow films at relatively low substrate temperature of $\sim 500\text{ }^{\circ}\text{C}$, as a high degree of ionization of all the species (deposition flux) provides the control of ion energy, allowing the films to grow at relatively lower temperatures [11]. By using the advantage of the high-energy vapor phase deposition, PLD technique has also been employed to grow various MAX phase thin films. Here one can use a single stoichiometric bulk target of the desired MAX phase for ablation by high energy pulsed laser beam ($\sim\text{eV}$), generating the plasma and thereby the true stoichiometric transfer of all the species on the substrate surface and thus providing a high possibility in the formation of a single phase epitaxial films. By PLD, films are typically grown at $\sim 700\text{ }^{\circ}\text{C}$. Starting with the first attempt of Ti-Si-C thin film growth by PLD by Phani *et al.*, [14], till now several attempts have been made to grow MAX phase thin films as summarized later on, however further investigation is still required to achieve the highest-crystalline quality of films.

MAX PHASE THIN FILMS

1. M_2AX ($n=1$)

211 MAX phases are the first layered compound of the ternary MAX series, showing excellent metallic behavior and high sustainability in extreme environments (e.g. high temperature, corrosive, oxidizing). Their large c/a lattice constant ratio, makes the properties of the material

highly anisotropic [8]. A typical band structure calculation shows the reasonable amount of density of states (DOS) at the Fermi level (E_F) [15], with a majority of the charge carriers (p -type) coming from the Ti-3d orbitals (Fig. 2a). Therefore, growing thin films of 211 MAX phases became an interesting avenue among the materials synthesis community. Wilhelmsson *et al.*, for the first time reported the epitaxial growth of Ti_2AlC MAX phase thin film by using the magnetron sputtering deposition technique [16]. They grew films at ~ 900 °C on Al_2O_3 (0001) substrates with a ~ 20 nm TiC (111) seed buffer layer for improving the epitaxy, and measured the resistivity of ~ 44 $\mu\Omega$ -cm at room temperature. Later they also measured the hardness and Young's modulus of ~ 600 nm Ti_2AlC film and obtained the values of ~ 20 GPa, and ~ 260 GPa, respectively [17]. High current pulsed cathodic arc deposition method was employed by Rosén *et al.*, to grow epitaxial Ti_2AlC thin films on sapphire and they observed a (001) (Ti_2AlC) // (0001) (Al_2O_3), and (11-20) (Ti_2AlC) // (11-20) (Al_2O_3) epitaxial relationship by using high-resolution HRTEM [18]. Pshyk *et al.*, grew ~ 120 nm Ti_2AlC MAX phase thin films by using electron beam physical vapor deposition at 700 °C [19] and investigated structural, nano-mechanical and tribological properties and found the hardness and elastic modulus of ~ 4.8 GPa and ~ 182.5 GPa, respectively (Fig. 2b). The elastic modulus is found to be lower than in case of films grown by sputtering [17], possibly due to used low growth temperature (~ 700 °C), leading to the formation of solid solution of Al in TiC. Films also showed a very low coefficient of friction of ~ 0.3 , with applied load of ~ 500 μN (Fig. 2c). Frodelius *et al.*, tried to optimize the growth of the Ti_2AlC phase by sputtering and found that additional Ti flux is important to grow the stoichiometric 211 MAX phase [20]. Later they also studied the oxidation of Ti_2AlC film grown at ~ 500 °C, forming a TiO_xC_y layer at the surface [21]. This shows that high temperature is important to grow pure phase MAX films and also to obtain a good oxidation resistance. Electrical resistivity measurement by Mauchamp *et al.*, shows the anisotropic behavior with room temperature resistivity of ~ 36 $\mu\Omega$ -cm for Ti_2AlC thin films [15]. Ti_2AlC MAX phase was also deposited on cubic MgO (001) substrates by magnetron sputtering. However, the films were found to be polycrystalline with hexagonal laminar grain with lateral size between ~ 150 -400 nm [22]. Feng *et al.*, also found that high temperature annealing is important in the formation of high-quality Ti_2AlC phase thin films [23].

Regarding other 211 MAX phases, Högberg *et al.*, reported the growth of epitaxial Ti_2GeC thin films on Al_2O_3 (0001) substrates at ~ 1000 °C by using the magnetron sputtering technique

[24]. After that they also grew Ti_2AlN thin films and observed low electrical resistivity of $\sim 39 \mu\Omega\text{-cm}$, comparable to the bulk value [25]. Emmerlich *et al.*, reported the growth of Ti_2GeC and Ti_2SnC thin films showing low electrical resistivity of $\sim 15\text{-}50 \mu\Omega\text{-cm}$ [26]. Moreover, Ti_2GeC films show high carrier density of $\sim 3.5 \times 10^{27} \text{ m}^{-3}$ [27]. Beckers *et al.*, grew Ti_2AlN films on MgO (111) and Al_2O_3 (0001) substrates by reactive sputtering methods and found that film decomposes at $\sim 800 \text{ }^\circ\text{C}$, because of the onward diffusion of Al [28]. Nanolaminate Ti_2AlN thin films were also synthesized by the multilayer deposition of $\sim 4.5 \text{ nm}$ Ti layers and $\sim 3 \text{ nm}$ thin AlN layers on $\text{Si}/\text{Si}_3\text{N}_4$ substrate and subsequent rapid thermal annealing [29]. A combined cathodic arc/sputter technique was also employed to grow dense and high-temperature stable Ti_2AlN MAX films [30].

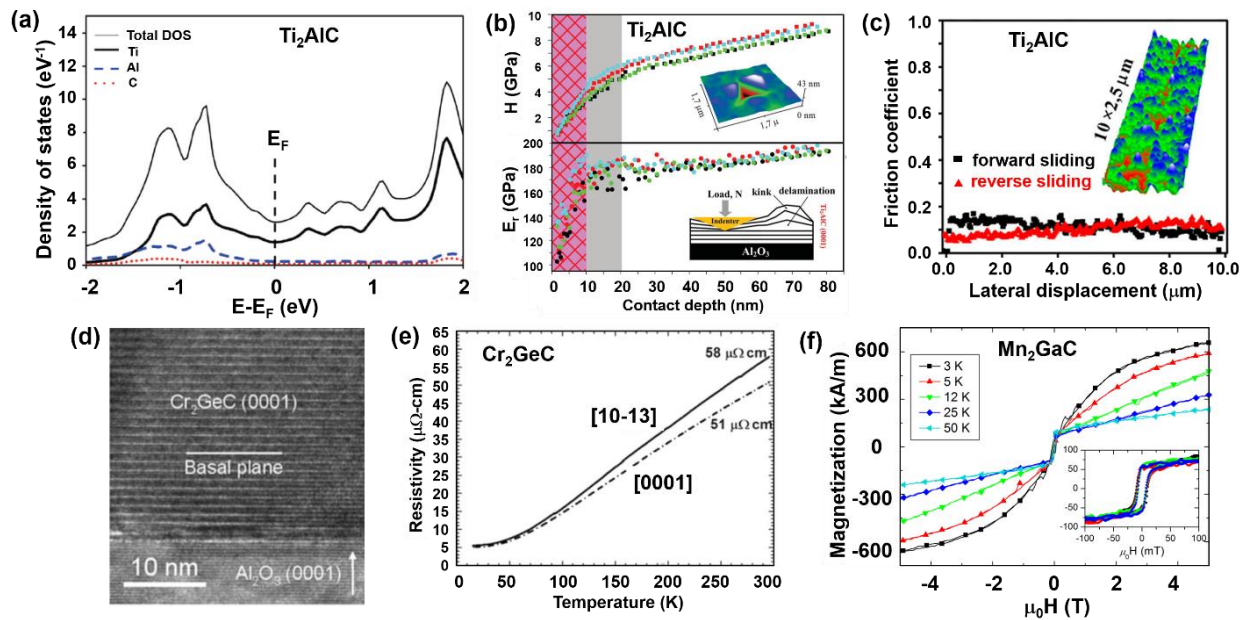


Figure 2: Properties of M_2AX ($n=1$) phases: (a) Theoretical band structure calculation of Ti_2AlC shows the presence of non-zero density of states (DOS) at the Fermi level (E_F), with dominant contribution from Ti-3d orbitals. (b), (c) Hardness and elastic moduli vs. contact depth of a $\sim 120 \text{ nm}$ thick Ti_2AlC film grown on sapphire. Inset shows the scanning probe images after the nano-indentation depth of 10 mN . (d) High-resolution TEM image shows the epitaxial growth of Cr_2GeC thin films along the basal plane. (e) Resistivity measurement of a $\sim 190 \text{ nm}$ Cr_2GeC thin film on Al_2O_3 (0001) shows anisotropic metallic behavior. (f) In-plane magnetization measurement of $\sim 100 \text{ nm}$ Mn_2GaC thin film grown on MgO (111) shows the presence of ferromagnetic ordering below 230 K . Inset shows the clear magnetic hysteresis loop at different temperatures. Adapted

with permission from Mauchamp *et al.*, *Phys Rev B* 2013; **87**: 235105, copyright 2013 American Physical Society [15]; Pshyk *et al.*, *Mater Res Lett* 2019; **7**: 244–250, copyright 2019 The Author(s). Published by Informa UK Limited, trading as Taylor & Francis Group [19]; Eklund *et al.*, *Phys Rev B* 2011; **84**: 075424, copyright 2011 American Physical Society [32]; Dahlqvist *et al.*, *Phys Rev B* 2016; **93**: 014410, copyright 2016 American Physical Society [40].

Interestingly, Scabarozi *et al.*, grew Nb₂AlC thin film on sapphire by magnetron sputtering and remarkably, it shows the superconducting transition at ~440 mK [31]. This is a unique example of MAX phase thin films which shows superconductivity. Eklund *et al.*, investigated the epitaxial growth and electrical transport of ~190 nm Cr₂GeC thin film by growing them on Al₂O₃ (0001) substrate by sputtering [32]. Before the growth, a seed layer of TiN (111) was pre-deposited on sapphire. Pure-phase films were found to be epitaxial as confirmed by the HRTEM (Fig. 2d). Moreover, electrical transport shows anisotropic behavior with resistivity of ~51 μΩ-cm (along 0001) and ~58 μΩ-cm (along 10-13) (Fig. 2e). Later, Scabarozi *et al.*, doped V into the film and grew (Cr_{1-x}V_x)₂GeC and investigated the electronic and elastic properties [33]. It shows metal-like electrical conductivity with a resistivity of ~50 μΩ-cm, as well as a minimal effect on the elastic moduli even after alloying.

Cr₂AlC films were synthesized by depositing multilayers of Cr, C, and Al on Si/Si₃N₄ substrates showing reasonable mechanical properties [34]. Hopfeld *et al.*, measured the tribological properties of Cr₂AlC films, obtaining the friction coefficients ranging between ~0.30–0.70 [35]. Recently, epitaxial thin films of Cr₂AlC on MgO (111) and Al₂O₃ (0001) substrates by pulsed laser deposition show the thickness dependent semiconductor-like and metal-like behavior, suggesting a percolation thickness for the observation of electronic properties [36]. Very recently, dual phase Cr₂AlC thin films were grown on Si (100) substrate by magnetron sputtering showing excellent radiation-tolerance behavior, useful for future fusion and fission nuclear reactors [37]. Stelzer *et al.*, measured the high-temperature resistivity of polycrystalline Cr₂AlC thin films and observed the changes in resistivity due to the structural changes from amorphous to a hexagonal disordered solid solution structure and from the latter to MAX phase [38]. Jiang *et al.*, gave an effort to grow V₂AlC thin films by magnetron sputtering [39]. Dahlqvist *et al.*, grew Mn₂GaC thin films on MgO (111) substrates and investigated their magnetic properties, showing magnetically driven anisotropic structural changes and ferromagnetic ordering below ~230 K (Fig. 2f), with

robust intra-layer ferromagnetic spin coupling [40]. Considering the antiferromagnetic ground state of Cr₂GaC, Petruhins *et al.*, successfully synthesized thin films of this compound [41].

From another application point of view, Ti₂AuN thin films were obtained from Au-covered Ti₂AlN thin films grown via magnetron sputtering on Al₂O₃ (000 l) substrate and subsequent high-temperature annealing which induces the intercalation of noble metals into the MAX phase [42]. Considering the double metal cations at M-site, Azina *et al.*, sputtered a (Ti,Zr)₂AlC target on Al₂O₃(000 l) substrate and found the formation of (Ti,Zr)₂AlC solid solution MAX phase film as confirmed by HRTEM [43]. Interestingly, they also found that high substrate temperature (≥ 950 °C) is necessary to form single phase (Ti,Zr)₂AlC thin film [44]. Mockute *et al.*, grew nanolaminated (Cr,Mn)₂AlC thin films on Al₂O₃ (0001) by sputtering [45]. Meshkian *et al.*, synthesized high-quality (Mo_{0.5}Mn_{0.5})₂GaC thin films on MgO (111) substrates, and performed the magnetic measurements showing a remanent magnetization (M_r) of ~ 0.35 μ_B /M-atom at low temperature (hence ferromagnetism) [46]. This is the largest reported value among MAX compounds, till date. Later, (Cr_{0.5}Mn_{0.5})₂GaC films were grown by Petruhins *et al.*, on MgO (111), 4H-SiC (0001), and Al₂O₃ (0001) with and without a NbN (111) seed layer, and they observed net magnetic moment of ~ 0.67 μ_B /(Cr + Mn) atom at ~ 30 K and magnetic field of 5 Tesla [47]. Moreover, Salikhov *et al.*, measured the ferromagnetic resonance spectra of the same film, showing negligible magneto-crystalline anisotropy [48]. These excellent properties of 211 MAX phase thin films shows its enormous potential for wide-range of electrical, mechanical, thermal applications, even in high energy nuclear fusion reactors.

2. M₃AX₂ ($n= 2$)

312 MAX phase has become an important class of materials because of its unique combination of excellent ceramic and metallic properties. As seen, similar to the 211 phases, for the 312 phases, the metallic nature is governed mostly by the contribution of Ti-3d orbitals (Fig. 3a) [49]. Also, the most intriguing properties of 312 phase is the etching out the A-layers, forming new 2D material MXenes. Therefore, several efforts have been given to synthesis new 312 phases, not only in its bulk form but also in its high quality epitaxial thin film form, a viable need for the applications. At an early stage, Goto and Hirai grew monolithic Ti₃SiC₂ poly-crystalline plates by CVD [50]. Racault *et al.*, also attempted to grow Ti₃SiC₂ thin films by CVD, however they obtained

mixed phase film [51]. Later Jacques *et al.*, modified the growth method and used pulsed reactive CVD to grow films, however the results came out to be the same [52]. Pickering *et al.*, also tried to deposit Ti_3SiC_2 by CVD, forming a mixed phase compound [53]. First epitaxial single-crystalline Ti_3SiC_2 thin film growth was reported by Palmquist *et al.*, where they grew films on MgO (111) substrates by sputtering techniques, at $\sim 900^\circ\text{C}$ [54]. They first grew a seed-layer of TiC (111), followed by the growth of Ti_3SiC_2 films, forming an epitaxy relation of Ti_3SiC_2 (0001)//TiC (111)//MgO (111), as confirmed by the cross-sectional TEM.

Emmerlich *et al.*, made an extensive structural characterizations about the formation of films. They also deposited few nm seed layer of TiC_x (111) to grow epitaxial layered Ti_3SiC_2 thin films by sputtering, as confirmed by HRTEM (Fig. 3b) [55]. Interestingly, even without the pre-deposition, they also found that a thin layer of TiC_x (111) was formed first on the MgO (111) substrate through the segregation of Si on top of the growth surface (Fig. 3c), relating to the complex growth kinetics and lattice relaxation mechanism, to minimize the high interfacial energy. Films with ~ 650 nm thickness shows very low electrical resistivity of $\sim 25 \mu\Omega\text{-cm}$ (on MgO (111)) and $\sim 33 \mu\Omega\text{-cm}$ (on Al_2O_3 (0001)). Films also show hardness of ~ 24 GPa and Young's modulus of $\sim 343\text{-}370$ GPa. Pécz *et al.*, found that formation of Ti_3SiC_2 phase via thermal evaporation of Al and Ti on *p*-type 6H-SiC (001) substrate and after annealing at $\sim 900^\circ\text{C}$ in a nitrogen ambient, with films showing excellent Ohmic contact behavior [56]. Later, Tsukimoto *et al.*, did microstructural characterizations of this structure by TEM and found a hetero-epitaxial orientation relationship of (0001) Ti_3SiC_2 // (0001) SiC and (0-110) Ti_3SiC_2 // (0-110) SiC [57]. In addition, Fashandi *et al.*, also investigated the excellent Ohmic contact behavior of the same multilayer by growing Ti_3SiC_2 by using a single-step procedure by sputter deposition of Ti on 4H-SiC at $\sim 960^\circ\text{C}$ [58]. Hopfeld *et al.*, measured the tribological properties of ~ 520 nm Ti_3SiC_2 thin films grown on Si (111) by magnetron sputtering and found the frictional coefficient value of $\sim 0.15\text{-}0.25$, making MAX useful as a lubricant material [35].

Hu *et al.*, grew ~ 200 nm Ti_3SiC_2 films by pulsed laser deposition on a polished silicon substrate at 100°C and 300°C and measured the mechanical properties, showing a friction coefficient of ~ 0.2 in humid air, and hardness of $\sim 30\text{-}40$ GPa [59]. Vishnyakov *et al.*, also deposited Ti_3SiC_2 at 650°C by magnetron sputtering technique on native oxide covered Si substrate and did the Raman spectroscopy showing two active Raman mode of E_{2g} ($\sim 622 \text{ cm}^{-1}$) and A_g ($\sim 657 \text{ cm}^{-1}$), arguing

that this could be a fast identification of the formation of 312 MAX phases [60]. Recently, one major breakthrough was made in MAX was the intercalation of noble metals Au or Ir into the ~60 nm-thick Ti_3SiC_2 films grown on 4H-SiC by sputtering, forming the highly crystalline atomically ordered novel Ti_3AuC_2 and Ti_3IrC_2 MAX phases, as confirmed by the HRTEM (inset of Fig. 3d) [61]. Remarkably, these structures show excellent Ohmic contact with SiC which was even retained after ~1000 hrs of aging at ~600 °C (Fig. 3d), making MAX useful for numerous high temperature electronic device applications.

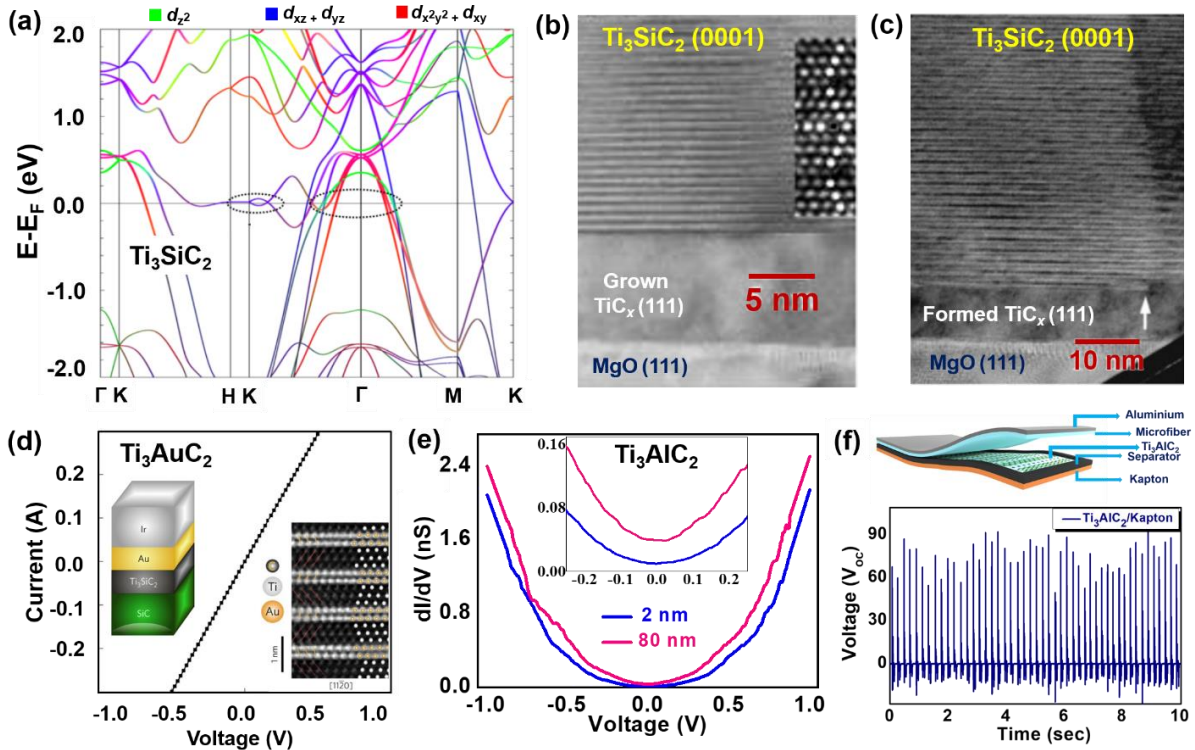


Figure 3: Properties of M_3AX_2 ($n=2$) phases: (a) Theoretical band structure of Ti_3SiC_2 shows metallic behavior with dominant contribution from the Ti-3d orbitals near the Fermi level. Atomic resolution TEM image of a layered Ti_3SiC_2 thin film with (b) an intentionally grown TiC_x (111) seed layer, and (c) without grown but formed TiC_x (111) seed layer during the deposition. (d) $\text{Ti}_3\text{AuC}_2/\text{SiC}$ shows a perfect Ohmic contact behavior, with a linear I - V characteristics, which are retained even after annealing for ~1000 hrs. Inset shows the schematic of iridium and gold covered Ti_3SiC_2 film grown on SiC and the atomic resolution TEM image of the layered Ti_3AuC_2 thin film, forming ordered structure after noble-metal exchange of A layers while annealing at high temperature. (e) Room temperature scanning tunneling microscopy (STM) I - V curve of Ti_3AlC_2

films on Al₂O₃ (0001) shows the metallic characteristics. (f) Triboelectric nano-generator device fabrication by using a metallic Ti₃AlC₂ film on flexible Kapton substrate as an electrode showing the peak-to-peak open-circuit voltage (V_{oc}) of ~80V, by applying a human mechanical force of ~15 N. Adapted with permission from Pinek *et al.*, *Phys Rev B* 2020; **102**: 075111, copyright 2020 American Physical Society [49]; Emmerlich *et al.*, *J Appl Phys* 2004; **96**: 4817 [55]; Fashandi *et al.*, *Nat Mater* 2017; **16**: 814, copyright 2017 Macmillan Publishers Limited, part of Springer Nature [61]; Biswas *et al.*, *Phys Rev Appl* 2020; **13**: 044705, copyright 2020 American Physical Society [65].

Regarding other well-known 312 compounds, Wilhelmsson *et al.*, grew epitaxial Ti₃AlC₂ thin films by magnetron sputtering on Al₂O₃ (0001) substrates, with a ~20 nm TiC_x (111) seed layer, showing resistivity, hardness and Young's modulus of ~51 μΩ-cm, ~20 GPa and ~260 GPa, respectively [16]. Magnuson *et al.*, deposited ~500 nm Ti₃AlC₂ films, ~200 nm Ti₃SiC₂ and Ti₃GeC₂ films by magnetron sputtering on Al₂O₃ (0001) substrate and investigated their electronic structures by soft x-ray emission spectroscopy [62]. Following the earlier reports, before the deposition of 312 phases, they also grew ~20 nm TiC_{0.7} (111) the buffer layer to promote high quality growth. Interestingly, they found that the differences in the electronic structure are strongly related to the bonding nature between Ti-C and Ti-A layers. Later, they also investigated the substrates temperature growth of these films and found that films grown at room temperature possess almost ~2.6 at% of oxygen content [63], which decreases with the increase in growth temperature. The film also shows room temperature resistivity of ~120 μΩ-cm. Högberg *et al.*, also grew these three films via a similar technique on Al₂O₃ (0001) as well as MgO (111) substrates, which shows room temperature resistivity of ~25-30 μΩ-cm, slightly higher than the reported bulk phase (~22 μΩ-cm), as a consequence of the possible thickness reduction for film case [25]. Nearly ~600 nm Ti₃AlC₂ phase was also synthesized by Wilhelmsson *et al.*, via magnetron sputtering on Al₂O₃ (0001) and they found hardness of ~20 GPa and Young's modulus of ~240 GPa [16]. Halim *et al.*, grew ~15 to 60 nm Ti₃AlC₂ thin film on (0001) sapphire substrate by magnetron sputtering and showed that films are highly conducting with room temperature resistivity of ~35-45 μΩ-cm with transparency of less than 30% [64]. Remarkably, they etched out the Al layer from the film and formed the transparent (~90%) conducting Ti₃C₂T_x MXene phase. Recently, we grew (103) oriented Ti₃AlC₂ thin film by pulsed laser deposition on Al₂O₃ (0001) substrates and investigated

various functional properties, showing metallic behavior as confirmed by scanning tunneling microscopy (**Fig. 3e**), and its usefulness as Ohmic contact, and transparent ultrathin conductor [65]. Moreover, by using Ti_3AlC_2 film as an electrode material for tribological bio-sensor based devices fabrication (**Fig. 3f**), the device shows high open-circuit output voltage (V_{oc}) upon applied human force, which might be very useful for biomechanical touch sensors for energy harvesting. Very recently, Torres *et al.*, also synthesized Ti_3AlC_2 thin films by thermal treatment of a Ti-Al-C multilayer system via magnetron sputtering and found resistivity, hardness and Young's modulus of $\sim 54 \mu\Omega\text{-cm}$, $\sim 3.2 \text{ GPa}$, and $\sim 120 \text{ GPa}$, respectively [66]. From magnetism point of view, Tao *et al.*, grew $(\text{V,Mn})_3\text{GaC}_2$ thin films by sputtering. Interestingly, this is the first synthesized magnetic MAX thin film among the 312 phase. Film shows the hysteretic $M-H$ loop between 50 K-300 K, indicating the possible presence of magnetic ordering well-above the room temperature [67] All these above observations point towards the remarkable application worthiness of 312 MAX phase thin films.

3. M_4AX_3 ($n= 3$) phase

Higher order ($n= 3$) 413 M_4AX_3 phase materials are also very interesting as they show high electrical conductivity, high damage tolerance, resistance to thermal shock, and high Young modulus. It possesses a very high out-of-plane lattice parameter of more than 20\AA . Theoretical calculation shows the presence of a considerable density of states (DOS) at the Fermi level (E_F) (**Fig. 4a**) [68]. Bulk Nb_4AlC_3 shows metallic behavior with room temperature resistivity of $\sim 75 \mu\Omega\text{-cm}$ with (**Fig. 4b**), with Vickers hardness of $\sim 2.6 \text{ GPa}$ (**Fig. 4c**) [69]. The bulk Ti_4AlN_3 shows Young's moduli of $\sim 310 \text{ GPa}$ (**Fig. 4d**) [70]. M_4AX_3 phases are also useful as a coating material on spacecraft to avoid solar heating as well as an increase in radiative cooling [68] because of the increase in thermal emittance as compared to the TiN phase as reflectivity decreases dramatically in the infrared region and increases in the region of visible light, due to lower plasma frequency. An atomic-scale Z-contrast TEM microstructure image of a 413 phase of polycrystalline $(\text{V}_{0.5}\text{Cr}_{0.5})_4\text{AlC}_3$ shows the ABABACBCBC stacking (**Fig. 4e**) [71]. Therefore, it would be extremely interesting to synthesize the relatively complex higher-order M_4AX_3 phase materials, both in bulk as well as in thin-film form.

As found in the literature, few efforts have been given to grow this complex 413 phase. Högberg *et al.*, grew Ti_4GeC_3 thin films on Al_2O_3 (0001) substrates by dc magnetron sputtering at $\sim 1000^\circ\text{C}$ which shows resistivity in the range of $\sim 50\text{-}200\ \mu\Omega\text{-cm}$ [24, 25]. Emmerlich *et al.*, grew Ti_4SiC_3 thin films on Al_2O_3 (0001) at temperatures ranging from ~ 500 to 950°C , by magnetron sputtering [26]. It was found that a thin layer of TiC_x (111) is formed due to initial Si segregation, as confirmed by XRD. The film shows room temperature resistivity of $\sim 51\ \mu\Omega\text{-cm}$, with a nominal effect from the TiC_x (111) seed layer at the film-substrate interface. Schramm *et al.*, obtained the Ti_4AlN_3 MAX phase by annealing the $(\text{Ti}_{1-x}\text{Al}_x)\text{N}_y$ thin films grown by reactive cathodic arc deposition [72]. They suggested that intercalation of Al and N along the basal plane accompanied by the simultaneous detwinning of the Ti_2AlN crystal leads to the formation of a higher-order Ti_4AlN_3 phase. Recently, Li *et al.*, grew a new Nb_4SiC_3 MAX phase thin films by magnetron sputtering on Si (001) substrates and evaluate their properties by using several techniques [73]. Films were found to be highly conducting with room temperature resistivity of $\sim 99\ \mu\Omega\text{-cm}$. It also shows high hardness and elastic moduli values of $\sim 15\ \text{GPa}$ and $\sim 200\ \text{GPa}$. Although the exploration of higher order M_4AX_3 phases is limited, probably because of the complexity in the synthesis of single-phase materials, however in the future, both theoretical insights about the growth and relevant experimental study will enrich the properties as well as possibly in tailoring the structure-property relationship in ever growing MAX phases.

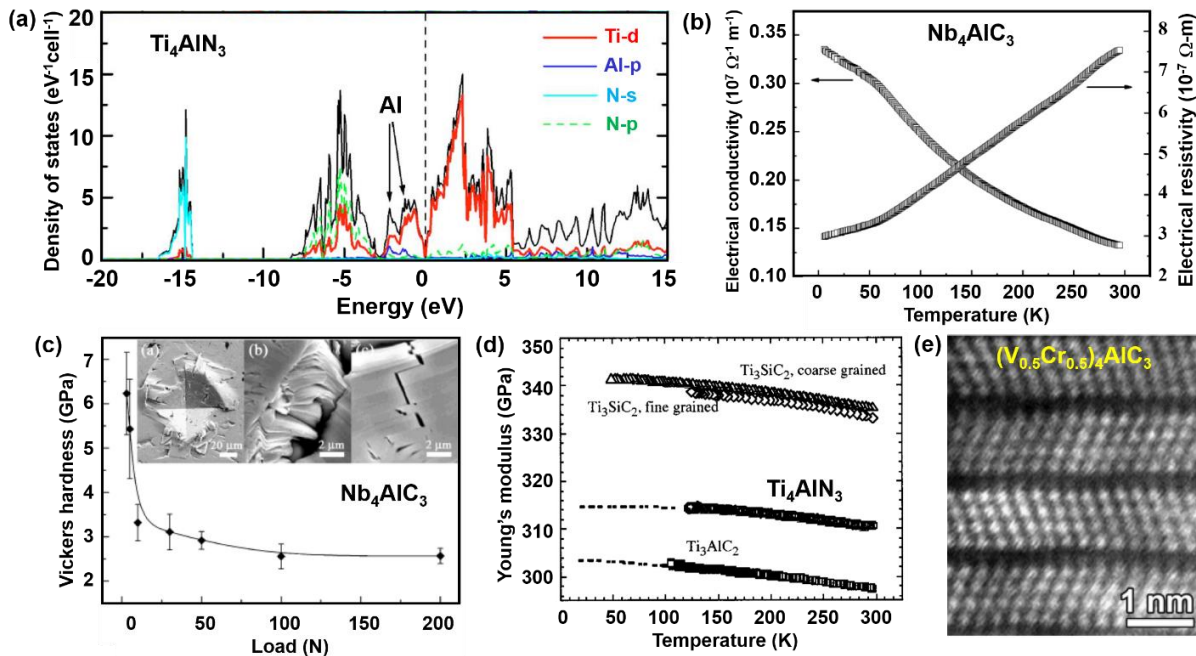


Figure 4: Properties of M_4AX_3 ($n=3$) phases: (a) Theoretical density of states (DOS) of Ti_4AlN_3 . (b) Temperature dependent electrical resistivity of bulk Nb_4AlC_3 showing metallic behavior. (c) Vickers hardness as a function of indentation loads for bulk Nb_4AlC_3 . Inset shows the SEM images at a different stage of the loads. (d) Temperature dependent Young's modulus of Ti_4AlN_3 . (e) High-resolution Z-contrast TEM image of polycrystalline $(V_{0.5}Cr_{0.5})_4AlC_3$ along [1-210] direction. Due to the unavailability of high-quality epitaxial thin film growth and consequent functional properties, here we have only shown the excellent property potentials of bulk 413 MAX phase. Adapted with permission from Li *et al.*, *Appl Phys Lett* 2008; **92**: 221907, copyright 2008 American Institute of Physics [68]; Finkel *et al.*, *J Appl Phys* 2000; **87**: 1701, copyright 2000 American Institute of Physics [70]; Hu *et al.*, *J Am Ceram Soc* 2008; **91**: 2258, Zhou *et al.*, *J Am Ceram Soc* 2008; **91**: 1357, copyright 2008 The American Ceramic Society [69, 71].

CONCLUSION AND OUTLOOK

In the last couple of decades several attempts have been made to grow high-quality epitaxial thin films of diverse ($n = 1-3$) MAX phases on various substrates by using different vapour phase deposition techniques (listed in [Table 2-4](#)). Films are mostly grown at high temperatures ($\sim 700-900$ °C), an important parameter to grow high quality epitaxial single-phase MAX phase films. Remarkably, these films show very high electrical and thermal conductivity, high Vickers hardness and Young's modulus, excellent corrosion and oxidation resistance, low frictional force, high thermal and radiation damage tolerance that might be extremely useful for consequent application domains. Although substantial progress has been made, however considering the synthesis of a large number of bulk MAX phase compounds, thin film growth of MAX has a long way to go and there remain several difficulties and changes to solve in the future, and these are the following:

1. First of all, one needs to grow epitaxial single crystalline MAX phase thin films directly on structurally compatible substrates, without the pre-growth of a thin TiC_x (111) seed layer, as it not only involves additional growth procedure but also contributes to the functional property measurements (however mere it is, having electrical resistivity of ~ 250 $\mu\Omega$ -cm), complicating in figuring out the actual contribution from the desired MAX film.
2. Low temperature growth without any surface oxidation is important as many times inter-diffusion between the elements from the substrate and of MAX film happens at a higher

temperature, forming abrupt interfaces and mixed phases, hence deteriorating the film quality and consequent functional properties. In addition, growth of MAX films at different substrate temperatures would also be very interesting, considering the complex structures and consequent growth-temperature dependent changes in functional properties.

3. Considering the extensive lists of bulk MAX phases with highly anisotropic properties, it is always important and useful to grow new stable/metastable thin films, not only along out-of-plane (000 l) orientations, but also along non-basal planes by epitaxy engineering, to widen the horizon of MAX with unforeseeable emergent properties.
4. MAX films are highly conducting as listed above, however tuning the band gap and making them semi-conducting-like and if possible, transparent too (via chemical doping/strain engineering/ultrathin films) would be important for the semiconductor industry as well as in photovoltaic technology.
5. Although some attempts have been given on finding magnetic MAX [74], however, growth of MAX thin films showing room-temperature ferro/anti-ferromagnetic ordering with high magnetic moment would be useful for spintronic applications.
6. The growth of ferroelectric MAX phase thin films would be useful for non-volatile memory device applications.
7. Growth of novel MAX phase films (e.g. high T_c superconductors, topological insulators, quantum Hall effect etc.) for exotic quantum/topological applications.
8. Unfortunately, MAX lacks its application potential as a good catalyst for electrochemical hydrogen energy productions. Considering the cost-effectiveness, it would be very useful to engineer the film and making MAX as a high performance catalysts, which can eventually replace the expensive noble metal Pt or Ir catalyst, currently used for renewable energy productions.
9. Considering the surface oxidation problem, synthesizing new MAX phases, not only in thin film form but also as bulk materials containing the X-element other than C or N, would be of extreme importance. This looks a promising new direction as Boron (B) based material has been synthesized, named as MAB phase [75].
10. Finally, last but not the least, considering the advancement in thin film growth technology, in the future, integrating MAX with well-developed functional metal-oxide thin films, thus making a synergy between layered non-oxide and oxide heterostructures [76], would open

up an entirely new avenue for emergent functionalities and technologically relevant next-generation applications.

Table 2: Growth and properties of M_2AX ($n=1$) phase thin films

Material	Method	Property	Reference
Ti ₂ AlC	Magnetron sputtering	Anisotropic electrical resistivity	[15]
Ti ₂ AlC	Magnetron sputtering	Low resistivity (~44 μΩ-cm)	[16]
Ti ₂ AlC	Magnetron sputtering	Epitaxial growth	[17]
Ti ₂ AlC	Pulsed cathodic arc	Epitaxial growth	[18]
Ti ₂ AlC	Electron beam physical vapor deposition	Low friction coefficient	[19]
Ti ₂ AlC	Magnetron sputtering	Epitaxial growth	[20]
Ti ₂ AlC	Magnetron sputtering	Good oxidation resistance	[21]
Ti ₂ AlC	Magnetron sputtering	Hexagonal laminal grains (~150-400 nm)	[22]
Ti ₂ AlC	Magnetron sputtering	High temperature formed crystalline phase	[23]
Ti ₂ GeC	Magnetron sputtering	Young's modulus (~300 GPa)	[24]
Ti ₂ AlN, Ti ₂ AlC	Magnetron sputtering	Epitaxial growth	[25]
Ti ₂ AC (A = Si, Ge, Sn)	Magnetron sputtering	Low resistivity (~20-50 μΩ-cm)	[26]
Ti ₂ GeC	Magnetron sputtering	Low resistivity (~30 μΩ-cm), <i>p</i> -type carrier (~3.5×10 ²⁷ m ⁻³)	[27]
Ti ₂ AlN	Magnetron sputtering	Al diffusion at high temperature	[28]
Ti ₂ AlN	Magnetron sputtering	High crystallinity and textured	[29]
Ti ₂ AlN	Combined cathodic arc/sputter technique	Dense film with high-stability	[30]
Nb ₂ AlC	Magnetron sputtering	Superconductivity at ~440 mK	[31]
Cr ₂ GeC	Magnetron sputtering	Low resistivity (~53-66 μΩ-cm) with anisotropic electron-phonon coupling	[32]
(Cr _{1-x} V _x) ₂ GeC	Magnetron sputtering	Metal-like electrical conductivity	[33]
Cr ₂ AlC	Magnetron sputtering	Excellent mechanical properties	[34]
Ti ₂ AlN and Cr ₂ AlC	Magnetron sputtering	Friction coefficient (~0.15 to 0.50) and (~0.30 to 0.70)	[35]
Cr ₂ AlC	PLD	Thickness dependent semiconductor-like and metallic-like behavior	[36]
Cr ₂ AlC	Magnetron sputtering	Dual phase film with	[37]

		radiation-tolerant	
Cr ₂ AlC	Magnetron sputtering	Amorphous film and induced resistivity change	[38]
V ₂ AlC	Magnetron sputtering	Structure analysis	[39]
Mn ₂ GaC	Magnetron sputtering	Robust intra-layer ferromagnetic spin coupling	[40]
Cr ₂ GaC	Magnetron sputtering	Thin film growth	[41]
Ti ₂ AuN	Magnetron sputtering	Noble metals inter-diffusion	[42]
(Ti,Zr) ₂ AlC	Magnetron sputtering	High temperature nucleation and growth of aluminides	[43]
(Ti,Zr) ₂ AlC	Magnetron sputtering	High temperature for single phase growth	[44]
(Cr,Mn) ₂ AlC	Magnetron sputtering	High-quality growth	[45]
(Mo _{0.5} Mn _{0.5}) ₂ GaC	Magnetron sputtering	Ferromagnetism at low T (M _r ~0.35 μB/M-atom)	[46]
(Cr _{0.5} Mn _{0.5}) ₂ GaC	Magnetron sputtering	Ferromagnetic behavior between 30-300 K (M _s ~0.67 μB/(Cr + Mn))	[47]
(Cr _{0.5} Mn _{0.5}) ₂ GaC	Magnetron sputtering	Absence of magneto-crystalline anisotropy	[48]

Table 3: Growth and properties of M₃AX₂ (n=2) phase thin films

Material	Method	Property	Reference
Ti ₃ AlC ₂	Magnetron sputtering	Low resistivity (~51 μΩ-cm), high hardness (~20 GPa), Young Modulus (~260 GPa)	[16]
Ti ₃ AlC ₂	Magnetron sputtering	Epitaxial growth	[17]
Ti ₃ GeC ₂	Magnetron sputtering	Low resistivity (~50 μΩ-cm)	[24]
Ti ₃ SiC ₂ , Ti ₃ GeC ₂ , Ti ₃ AlC ₂	Magnetron sputtering	Low resistivity (~30-39 μΩ-cm), hardness (~15-25 GPa)	[25]
Ti ₃ SiC ₂	Magnetron sputtering	Friction coefficient (~0.15 -0.25)	[35]
Ti ₃ SiC ₂	CVD	Poly-crystalline plates	[50]
Ti ₃ SiC ₂	CVD	Mixed phase	[51]
Ti ₃ SiC ₂	Reactive CVD	Mixed phase	[52]
Ti ₃ SiC ₂	CVD	Mixed phase	[53]
Ti ₃ SiC ₂	Magnetron sputtering	Epitaxial growth	[54]
Ti ₃ SiC ₂	Magnetron sputtering	Low resistivity (~25 μΩ-cm), hardness (~24 GPa), modulus (~343-370 GPa)	[55]

Ti ₃ SiC ₂	CVD	Ohmic contact	[56]
Ti ₃ SiC ₂	CVD	Atomic structure	[57]
Ti ₃ SiC ₂	Magnetron sputtering	Ohmic contact	[58]
Ti ₃ SiC ₂	PLD	Low friction coefficient (~0.2 in humid air), and high hardness (~30 and 40 GPa)	[59]
Ti ₃ SiC ₂	Magnetron sputtering	Structural and Raman spectroscopy	[60]
Ti ₃ AuC ₂ , and Ti ₃ IrC ₂	CVD	High temperature stable Ohmic contact	[61]
Ti ₃ AC ₂ , (A= Al, Si, Ge)	Magnetron sputtering	Weak covalent bonding and charge transfer	[62]
Ti ₃ SiC ₂	Magnetron sputtering	Low resistivity (~120 μΩ-cm)	[63]
Ti ₃ AlC ₂	Magnetron sputtering	Low resistivity (~37-45 μΩ-cm)	[64]
Ti ₃ AlC ₂	PLD	Bottom electrode, Schottky diode, Ohmic contact, transparent conductor, biomechanical touch sensor	[65]
Ti ₃ AlC ₂	Magnetron sputtering	Low resistivity (~54 μΩ-cm), high hardness (~3.2 GPa)	[66]
(V,Mn) ₃ GaC ₂	Magnetron sputtering	Ferromagnetic between 50 to 300 K	[67]

Table 4: Growth and properties of M₄AX₃ (*n*=3) phase thin films

Material	Method	Property	Reference
Ti ₄ GeC ₃	Magnetron sputtering	Low resistivity (~50 μΩ-cm)	[24]
Ti ₄ SiC ₃	Magnetron sputtering	Low resistivity (~51 μΩ cm)	[26]
Ti ₄ AlN ₃	Reactive cathodic arc deposition	Micro-structural analysis	[72]
Nb ₄ SiC ₃	Magnetron Sputtering	Low resistivity (~99 μΩ-cm), high hardness (~15 GPa), Young Modulus (~200 GPa)	[73]

ACKNOWLEDGMENTS

A.B. would like to acknowledge the hospitality at RICE University.

AUTHORS' CONTRIBUTIONS

The manuscript was conceptualized by A.B. and written through the contributions of all authors. All authors have approved the final version of the manuscript.

CONFLICT OF INTEREST STATEMENT

There are no conflicts of interest to declare.

REFERENCES

1. Barsoum MW. The $M_{N+1}AX_N$ Phases: A New Class of Solids. *Prog Solid St Chem.* 2000; **28**: 201-280.
2. Barsoum MW, El-Raghy T. The MAX Phases: Unique New Carbide and Nitride Materials. *American Scientist* 2001; **89**, 334-343.
3. Radovic M, Barsoum MW, MAX phases: Bridging the gap between metals and ceramics. *Am Ceram Soc Bull* 2013; **92**: 20.
4. Fu L, Xia W. MAX Phases as Nanolaminate Materials: Chemical Composition, Microstructure, Synthesis, Properties, and Applications. *Adv Eng Mater* 2021; **23**: 2001191.
5. Gonzalez-Julian J. Processing of MAX phases: From synthesis to applications. *J Am Ceram Soc* 2021; **104**: 659–690.
6. Jeitschko W, Nowotny H, Benesovsky F. Kohlenstoffhaltige ternäre Verbindungen (H-Phase). *Monatshefte für Chemie und verwandte Teile anderer Wissenschaften* 1963; **94**: 672–676.
7. Barsoum MW, El-Raghy T. Synthesis and characterization of a remarkable ceramic: Ti_3SiC_2 . *J Am Ceram Soc* 1996; **79**: 1953-1956.
8. Sokol M, Natu V, Kota S, Barsoum MW. On the Chemical Diversity of the MAX Phases. *Trends in Chemistry* 2019; **1**: 210-223.
9. Naguib M, Barsoum MW, Gogotsi Y. Ten Years of Progress in the Synthesis and Development of MXenes. *Adv Mater* 2021; **33**: 2103393.

10. Hart JL, Hantanasirisakul K, Lang AC, Anasori B, Pinto D, Pivak Y, Tin van Omne J, May SJ, Gogotsi Y, Taheri ML. Control of MXenes' electronic properties through termination and intercalation. *Nat Commun* 2019; **10**: 522.
11. Eklund P, Beckers M, Jansson U, Högberg H, Hultman L. The $M_{n+1}AX_n$ phases: Materials science and thin-film processing. *Thin Solid Films* 2010; **518**: 1851–1878.
12. Arni S, Ingason SA, Petruhins A, Rosen J. Toward Structural Optimization of MAX Phases as Epitaxial Thin Films. *Mater Res Lett* 2016; **4**: 152-160.
13. Eklund P, Rosen J, Persson POÅ. Layered ternary $M_{n+1}AX_n$ phases and their 2D derivative MXene: an overview from a thin-film perspective. *J Phys D Appl Phys* 2017; **50**: 113001
14. Phani AR, Krzanowski JE, Nainaparampil JJ. Structural and mechanical properties of TiC and Ti–Si–C films deposited by pulsed laser deposition. *J Vac Sci & Tech A* 2001; **19**: 2252.
15. Mauchamp V, Yu W, Gence L, Piraux L, Cabioch T, Gauthier V, Eklund P, Dubois S. Anisotropy of the resistivity and charge-carrier sign in nanolaminated Ti_2AlC : Experiment and ab initio calculations. *Phys Rev B* 2013; **87**: 235105.
16. Wilhelmsson O, Palmquist JP, Nyberg T, Jansson U. Deposition of Ti_2AlC and Ti_3AlC_2 epitaxial films by magnetron sputtering. *Appl Phys Lett* 2004; **85**: 1066.
17. Wilhelmsson O, Palmquist JP, Lewina E, Emmerlich J, Eklund P, Persson POÅ, Högberg H, Li S, Ahuja R, Eriksson O, Hultman L, Jansson U. Deposition and characterization of ternary thin films within the Ti–Al–C system by DC magnetron sputtering, *J Cryst Growth* 2006; **291**: 290–300.
18. Rosén J, Ryves L, Persson POÅ, Bilek MMM, Deposition of epitaxial Ti_2AlC thin films by pulsed cathodic arc. *J Appl Phys* 2007; **101**: 056101.
19. Pshyk AV, Coy E, Kempinski EM, Scheibe B, Jurgaa S. Low-temperature growth of epitaxial Ti_2AlC MAX phase thin films by low-rate layer-by-layer PVD. *Mater Res Lett* 2019; **7**: 244–250.
20. Frodelius J, Eklund P, Beckers M, Persson POÅ, Högberg H, Hultman L. Sputter deposition from a Ti_2AlC target: Process characterization and conditions for growth of Ti_2AlC . *Thin Solid Films* 2010; **518**: 1621–1626.

21. Frodelius J, Lu J, Jensen J, Paul D, Hultman L, Eklund P, Phase stability and initial low-temperature oxidation mechanism of Ti₂AlC thin films. *J European Ceram Soc* 2013; **33**: 375–382.
22. Su R, Zhang H, O'Connor DJ, Shi L, Meng X, Zhang H. Deposition and characterization of Ti₂AlC MAX phase and Ti₃AlC thin films by magnetron sputtering. *Mater Lett* 2016; **179**: 194–197.
23. Feng Z, Ke P, Wang A. Preparation of Ti₂AlC MAX Phase Coating by DC Magnetron Sputtering Deposition and Vacuum Heat Treatment. *J Mater Sci & Tech* 2005; **31**: 1193–1197.
24. Högberg H, Eklund P, Emmerlich J, Birch J, L. Hultman. Epitaxial Ti₂GeC, Ti₃GeC₂, and Ti₄GeC₃ MAX-phase thin films grown by magnetron sputtering. *J Mater Res* 2005; **20**: 779.
25. Högberg H, Hultman L, Emmerlich J, Joelsson T, Eklund P, Molina-Aldareguia JM, Palmquist JP, Wilhelmsson O, Jansson U. Growth and characterization of MAX-phase thin films, *Surface & Coatings Technology* 2005; **193**: 6–10.
26. Emmerlich J, Eklund P, Rittrich D, Högberg H, Hultman L. Electrical resistivity of Ti_{n+1}AlC_n (A = Si, Ge, Sn, n = 1–3) thin films. *J Mater Res* 2007; **22**: 2279.
27. Scabarozi TH, Eklund P, Emmerlich J, Högberg H, Meehan T, Finkel P, Barsoum MW, Hettinge D, Hultman L, Lofland SE. Weak electronic anisotropy in the layered nanolaminate Ti₂GeC. *Solid State Commun* 2008; **146**: 498–501.
28. Beckers M, Schell N, Martins RMS, Mücklich A, Möller W. Phase stability of epitaxially grown Ti₂AlN thin films. *Appl Phys Lett* 2006; **89**: 074101.
29. Grieseler R, Kups T, Wilke M, Hopfeld M, Schaaf P. Formation of Ti₂AlN nanolaminate films by multilayer-deposition and subsequent rapid thermal annealing. *Mater Lett* 2012; **82**: 74–77.
30. Wang Z, Liu J, Wang L, Li X, Ke P, Wang A. Dense and high-stability Ti₂AlN MAX phase coatings prepared by the combined cathodic arc/sputter technique. *Appl Surf Sci* 2017; **396**: 1435–1442.
31. Scabarozi TH, Roche J, Rosenfeld A, Lim SH, Salamanca-Riba L, Yong G, Takeuchi I, Barsoum MW, Hettinger JD, Lofland SE. Synthesis and characterization of Nb₂AlC thin films. *Thin Solid Films* 2009; **517**: 2920–2923.

32. Eklund P, Bugnet M, Mauchamp V, Dubois S, Tromas T, Jensen J, Piraux L, Gence L, Jaouen M, Cabioch T. Epitaxial growth and electrical transport properties of Cr₂GeC thin films. *Phys Rev B* 2011; **84**: 075424.
33. Scabarozzi TH, Benjamin S, Adamson B, Applegate J, Roche J, Pfeiffer E, Steinmetz C, Lunk C, Barsoum MW, Hettinger JD, Lofland SE. Combinatorial investigation of the stoichiometry, electronic transport and elastic properties of (Cr_{1-x}V_x)₂GeC thin films. *Scripta Materialia* 2012; **66**: 85–88.
34. Grieseler R, Hähnlein B, Stubenrauch M, Kups T, Wilke M, Hopfeld M, Pezoldt J, Schaaf P, Nanostructured plasma etched, magnetron sputtered nanolaminar Cr₂AlC MAX phase thin film. *Appl Surf Sci* 2014; **292**: 997– 1001.
35. Hopfeld M, Grieseler R, Vogel A, Romanus H, Schaaf P. Tribological behavior of selected M_{n+1}AX_n phase thin films on silicon substrates. *Surface & Coatings Technology* 2014; **257**: 286–294.
36. Stevens M, Pazniak H, Jemiola A, Felek M, Farl M, Wiedwald U. Pulsed laser deposition of epitaxial Cr₂AlC MAX phase thin films on MgO(111) and Al₂O₃(0001). *Mater Res Lett* 2021; **9**: 343-349.
37. Tunes MA, Imtyazuddin M, Kainz C, Pogatscher S, Vishnyakov VM. Deviating from the pure MAX phase concept: Radiation-tolerant nanostructured dual-phase Cr₂AlC. *Sci Adv* 2021; **7**: eabf6771.
38. Stelzer B, Chen X, Bliem P, Hans M, Völker B, Sahu R, Scheu C, Primetzhofer D, Schneider JM. Remote Tracking of Phase Changes in Cr₂AlC Thin Films by In-situ Resistivity Measurements. *Sci Rep* 2019; **9**: 266.
39. Jiang Y, Mráz S, Schneider JM. Growth of V–Al–C thin films by direct current and high power impulse magnetron sputtering from a powder metallurgical composite target. *Thin Solid Films* 2013; **538**:1–6.
40. Dahlqvist M, Ingason AS, Alling B, Magnus F, Thore A, Petruhins A, Mockute A, Arnalds UB, Sahlberg M, Hjörvarsson B, Abrikosov IA, Rosen J. Magnetically driven anisotropic structural changes in the atomic laminate Mn₂GaC. *Phys Rev B* 2016; **93**: 014410.
41. Petruhins A, Ingason AS, Dahlqvist M, Mockute A, Junaid M, Birch J, Lu J, Hultman L, Persson POÅ, Rosen J. Phase stability of Cr_{n+1}GaC_n MAX phases from first principles and

Cr₂GaC thin-film synthesis using magnetron sputtering from elemental targets. *Phys Status Solidi RRL* 2013; **7**: 971–974.

42. Kashiwaya S, Lai C, Lu J, Petruhins A, Rosen J, Hultman L. Formation of Ti₂AuN from Au-Covered Ti₂AlN Thin Films: A General Strategy to Thermally Induce Intercalation of Noble Metals into MAX Phases. *Cryst Growth Des* 2020; **20**: 4077–4081.
43. Azina C, Tunca B, Petruhins A, Xin B, Yildizhan M, Persson POÅ, Vleugels J, Lambrinou K, Rosen J, Eklund P. Deposition of MAX phase-containing thin films from a (Ti,Zr)₂AlC compound target. *Appl Surf Sci* 2021; **551**:149370.
44. Azina C, Euland P. Effects of temperature and target power on the sputter-deposition of (Ti,Zr)_{n+1}AlC_n MAX-phase thin films. *Results in Materials* 2021; **9**: 100159.
45. Mockute A, Dahlqvist M, Emmerlich J, Hultman L, Schneider JM, Persson POÅ, Rosen J. Synthesis and ab initio calculations of nanolaminated (Cr,Mn)₂AlC compounds. *Phys Rev B* 2013; **87**: 094113.
46. Meshkian M, Ingason AS, Arnalds UB, Magnus F, Lu J, Rosen J. A magnetic atomic laminate from thin film synthesis: (Mo_{0.5}Mn_{0.5})₂GaC. *APL Mater* 2015; **3**: 076102.
47. Petruhins A, Ingason AS, Lu J, Magnus F, Olafsson S, Rosen J. Synthesis and characterization of magnetic (Cr_{0.5}Mn_{0.5})₂GaC thin films. *J Mater Sci* 2015; **50**: 4495–4502.
48. Salikhov R, Semisalova AS, Petruhins A, Sigurdur A, Rosen IJ, Wiedwald U, Farle M. Magnetic Anisotropy in the (Cr_{0.5}Mn_{0.5})₂GaC MAX Phase. *Mater Res Lett* 2015; **3**: 156-160.
49. Pinek D, Ito T, Furuta K, Kim Y, Ikemoto M, Ideta S, Tanaka K, Nakatake M, Fèvre PL, Bertran F, Ouisse T. Near Fermi level electronic structure of Ti₃SiC₂ revealed by angle-resolved photoemission spectroscopy. *Phys Rev B* 2020; **102**: 075111.
50. Goto T, Hirai T. Chemically vapor deposited Ti₃SiC₂. *Mater Res Bull* 1987; **22**: 1195-1201.
51. Racault C, Langlais F, Naslain R. On the chemical vapour deposition of Ti₃SiC₂ from TiCl₄-SiCl₄-CH₄-H₂ gas mixtures. *J Mater Sci* 1994; **29**: 3941-3948.
52. Jacques S, Di-Murro H, Berthet MP, Vincent H. Pulsed reactive chemical vapor deposition in the C-Ti-Si system from H₂/TiCl₄/SiCl₄. *Thin Solid Films* 2005; **478**:13-20.
53. Pickering E, Lackey WJ, Crain S. CVD of Ti₃SiC₂. *Chemical Vapor Deposition* 2000; **6**: 289-295.

54. Palmquist JP, Jansson U, Seppänen T, Persson POÅ, Birch J, Hultman L, Isberg P. Magnetron sputtered epitaxial single-phase Ti_3SiC_2 thin films. *Appl Phys Lett* 2002; **81**: 835.
55. Emmerlich J, Högberg H, Sasvári S, Persson POÅ, Hultman L, Palmquist J, Jansson U, Molina-Aldareguia JM, Czigány Z, Growth of Ti_3SiC_2 thin films by elemental target magnetron sputtering. *J Appl Phys* 2004; **96**: 4817.
56. Pécz B, Tóth L, di Forte-Poisson MA, Vacas J. Ti_3SiC_2 formed in annealed Al/Ti contacts to *p*-type SiC. *Appl Surf Sci* 2003; **206**: 8-11.
57. Tsukimoto S, Ito K, Wang Z, Saito M, Ikuhara Y, Murakami M. Growth and Microstructure of Epitaxial Ti_3SiC_2 Contact Layers on SiC. *Materials Transactions*, 2009; **50**: 1071- 1075.
58. Fashandi H, Andersson M, Eriksson J, Lu J, Smedfors K, Zetterling CM, Spetza AL, Eklund P. Single-step synthesis process of Ti_3SiC_2 ohmic contacts on 4H-SiC by sputter-deposition of Ti. *Scripta Materialia* 2015; **99**: 53–56.
59. Hu JJ, Bultman JE, Patton S, Zabinski JS. Pulsed laser deposition and properties of $M_{n+1}AX_n$ phase formulated Ti_3SiC_2 thin films. *Tribology Letters* 2004; **16**: 113.
60. Vishnyakov V, Lub J, Eklund P, Hultman L, Colligon J. Ti_3SiC_2 -formation during Ti-C-Si multilayer deposition by magnetron sputtering at 650 °C. *Vacuum* 2013; **93**:56-59.
61. Fashandi H, Dahlqvist M, Lu J, Palisaitis J, Simak SI, Abrikosov IA, Rosen J, Hultman L, Andersson M, Spetz AL, Eklund P. Synthesis of Ti_3AuC_2 , $Ti_3Au_2C_2$ and Ti_3IrC_2 by noble metal substitution reaction in Ti_3SiC_2 for high-temperature-stable Ohmic contacts to SiC. *Nat Mater* 2017; **16**: 814.
62. Magnuson M, Palmquist JP, Mattesini M, Li S, Ahuja R, Eriksson O, Emmerlich J, Wilhelmsson O. Eklund P, Högberg H, Hultman L, Jansson U, Electronic structure investigation of Ti_3AlC_2 , Ti_3SiC_2 , and Ti_3GeC_2 by soft x-ray emission spectroscopy. *Phys Rev B* 2005; **72**: 245101.
63. Magnuson M, Tengdelius L, Greczynski G, Eriksson F, Jensen J, Lu J, Samuelsson M, Eklund P, Hultman L, Högberg H. Compositional dependence of epitaxial $Ti_{n+1}SiC_n$ MAX-phase thin films grown from a Ti_3SiC_2 compound target. *J Vac Sci & Tech A* 2019; **37**: 021506.

64. Halim J, Lukatskaya MR, Cook KM, Lu J, Smith CR, Näslund L, May SJ, Hultman L, Gogotsi Y, Eklund P, Barsoum MW. Transparent Conductive Two-Dimensional Titanium Carbide Epitaxial Thin Films. *Chem Mater* 2014; **26**: 2374–2381.
65. Biswas A, Sengupta A, Rajput U, Singh SK, Antad V, Hossain SM, Parmar S, Rout D, Deshpande A, Nair S, Ogale S. Growth, Properties, and Applications of Pulsed Laser Deposited Nanolaminate Ti_3AlC_2 Thin Films. *Phys Rev Appl* 2020; **13**: 044075.
66. Torres C, Quispe R, Calderón NZ, Eggert L, Hopfeld M, Rojas C, Camargo MK, Bund A, Schaaf P, Grieseler R, Development of the phase composition and the properties of Ti_2AlC and Ti_3AlC_2 MAX-phase thin films – A multilayer approach towards high phase purity. *Appl Surf Sci* 2021; **537**: 147864.
67. Tao Q, Salikhov R, Mockute A, Lu J, Farle M, Wiedwald U, Rosen J. Thin film synthesis and characterization of a chemically ordered magnetic nanolaminate $(\text{V},\text{Mn})_3\text{GaC}_2$. *APL Mater* 2016; **4**: 086109.
68. Li S, R. Ahuja R, Barsoum MW, Jena P, Johansson B. Optical properties of Ti_3SiC_2 and Ti_4AlN_3 . *Appl Phys Lett* 2008; **92**: 221907.
69. Hu C, Li F, He L, Liu M, Zhang J, Wang J, Bao Y, Wang J, Zhou Y. In Situ Reaction Synthesis, Electrical and Thermal, and Mechanical Properties of Nb_4AlC_3 . *J Am Ceram Soc* 2008; **91**: 2258–2263.
70. Finkel P, Barsoum MW, El-Raghy T. Low temperature dependencies of the elastic properties of Ti_4AlN_3 , $\text{Ti}_3\text{Al}_{1.1}\text{C}_{1.8}$, and Ti_3SiC_2 . *J Appl Phys* 2000; **87**: 1701.
71. Zhou Y, Meng F, Zhang J. New MAX-Phase Compounds in the V–Cr–Al–C System. *J Am Ceram Soc* 2008; **91**: 1357–1360.
72. Schramm IC, Pauly C, Joesaar MPJ, Eklund P, Schmauch J, Mücklich F, Oden M. Solid state formation of Ti_4AlN_3 in cathodic arc deposited $(\text{Ti}_{1-x}\text{Al}_x)\text{N}_y$ alloys. *Acta Materialia* 2017; **129**: 268e277.
73. Li Z, Liu G, Liu G, Zhu X, Fu Y. Deposition of Nb-Si-C Thin Films by Radio Frequency Magnetron Sputtering. *Coatings* 2021; **11**: 524.
74. Ingason AS, Dahlgqvist M, Rosen J. Magnetic MAX phases from theory and experiments; a review. *J Phys Condens Matter* 2016; **28**: 433003.
75. Kota S, Sokol M, Barsoum MW. A progress report on the MAB phases: atomically laminated, ternary transition metal borides. *Inter Mater Rev* 2020; **65**: 226-255.

76. Kang KT, Park J, Suh D, Choi WS, Synergetic behavior in 2D layered material/complex oxide heterostructures, *Adv Mater* 2019; **31**: 1803732.